Infocommunications and Radio Technologies, vol. 4, no. 4, pp. 279–291, 2021.
Инфокоммуникационные и радиоэлектронные технологии. 2021. Т. 4, № 4. С. 279—291.
ISSN: 2587-9936

Analysis of a Vacuum Resonant-Tunneling Triode

M. V. Davidovich, G. N. Kolesov, and K. A. Sayapin

Institute of physics, Saratov State University
83, Astrakhanskaya str., Saratov, 410012, Russian Federation
davidovichmv@info.sgu.ru

Received: April 25, 2021
Peer-reviewed: September 16, 2021
Accepted: September 16, 2021

Abstract: *Stationary and non-stationary models are proposed for calculating the tunneling current of a vacuum resonant-tunneling triode with a control grid. The stationary model is based on the solution of the stationary Schrodinger equation by the matrix method with the calculation of the potential profile in a structure having several electrodes by the method of multiple images.*

Keywords: *tunneling, field emission, resonant tunnel transistor, Schrodinger equation, Poisson equation.*

For citation (IEEE): M. Davidovich, G. Kolesov, and K. Sayapin, “Analysis of a Vacuum Resonant-Tunneling Triode”, *Infocommunications and Radio Technologies*, vol. 4, no. 4, pp. 279–291, 2021.

УДК 621.38

Анализ вакуумного резонансно-туннельного триода

Давидович М. В., Колесов Г. Н., Саяпин К. А.

[1] *Институт физики, Саратовский государственный университет*
Саратов, 410012, Российская Федерация

Получено: 25 апреля 2021 г.
Отрецензировано: 16 сентября 2021 г.
Принято к публикации: 16 сентября 2021 г.

Аннотация: *Предложены стационарная и нестационарная модели расчета туннельного тока вакуумного резонансно-туннельного триода с управляющей сеткой. Стационарная модель основана на решении стационарного уравнения Шрёдингера матричным методом и методом множественных изображений с расчетом профиля потенциала в конструкции, имеющей несколько электродов.*

Ключевые слова: *туннелирование, автоэлектронная эмиссия, резонансный туннельный транзистор, уравнение Шрёдингера, уравнение Пуассона.*

Для цитирования (ГОСТ 7.0.5—2008): Давидович М. В., Колесов Г. Н., Саяпин К. А. Анализ вакуумного резонансно-туннельного триода // Инфокоммуникационные и радиоэлектронные технологии. 2021. Т. 4, № 4. С. 279—291.

Для цитирования (ГОСТ 7.0.100—2018): Давидович, М. В. Анализ вакуумного резонансно-туннельного триода / М. В. Давидович, Г. Н. Колесов, К. А. Саяпин // Инфокоммуникационные и радиоэлектронные технологии. — 2021. — Т. 4, № 4. — С. 279—291.

1. Introduction

The vacuum tunnel triodes are very interesting objects of research for vacuum microelectronics, since they do not require incandescence for operation, and the emission structure can be very compact and at the same time create very large currents necessary for the operation of devices. Such resonant tunnel transistors (RTTs) can be used as emission sources with a high current density. For this purpose, triodes with a double grid and a grid in the form of several conducting layers separated by vacuum gaps are interesting. Such grids are able to create a multi-humped quasi-periodic potential barrier that can be transparent in a certain energy band. In addition to resonant tunnel diodes (RTDs), the multi-barrier (multi-hump) resonant tunnel heterostructures also are used in nanoelec-

tronics, for example, in quantum cascade lasers. In contrast, vacuum RTTs in the form of heterostructures are convenient for current control. In this paper, for these purposes, the vacuum RTT is studied under stationary consideration. The stationary Schrodinger equation (SE) is solved and the VAC is calculated.

According to the Fowler–Nordheim formula, field or autoelectronic emission (AE) is theoretically capable of providing gigantic current densities of the order of $J \sim 10^{15}$ A/m^2 or more (depending on the concentration of free electrons in the cathode), but under the action of very strong fields [1, 2]. At such fields, the potential barrier practically disappears, and almost all the electrons tunnel that run into the cathode surface. However, very strong fields lead to a number of negative effects, such as reverse bombardment of the cathode, heating of the cathode, explosive emission, ponderomotor forces. Therefore, a promising direction is to increase the current density at not too strong fields. This is possible with resonant tunneling. Another effect that increases the current is associated with the penetration of the field deep into the cathode and with a change in the shape and thickness of the barrier in the cathode region. This can be achieved by making a thin dielectric or semiconductor film with a thickness of several nanometers on the cathode surface, or by making a cathode with a porous carbon structure from various allotropic carbon modifications [3-9]. As the latter, carbon nanoclusters made of diamond and graphite phases are convenient [3-9]. The field penetrates into the considered structures with a weakening, as a result of which the barrier thickness decreases by an order of magnitude of the film thickness. Its height is also slightly reduced. These are dimensional effects. The penetration of the field into the cathode to a depth of several nm leads to an acceleration of the electrons incident on its surface, an increase in their energy and better tunneling. In addition, when using clusters with dielectric and metallic (semiconductor) phases, Tamm levels appear on their surfaces, which promote tunneling. Their presence manifests itself as a hysteresis when the applied voltage changes over time [8].

Resonant tunnel structures based on semiconductors are performed by doping. The semiconductor resonant-tunnel transistor (RTT) and RTD can form a double-humped potential barrier and a VAC with incident sections, and are widely used as amplifiers and generators of the THz range. For vacuum RTT, it is necessary to isolate the grid from the cathode with a vacuum gap. If such a grid is in contact with the cathode, Fig. 1, then another insulated grid is required. If both meshes are isolated and are under certain potentials, such a structure can be considered as a tetrode. If one of the grids is grounded (contacts the cathode), or two grids are connected, then it is a triode. Two additional electrodes to the cathode and anode make it possible to create a three-humped po-

tential barrier with local levels between the humps, providing resonant tunneling Fig. 2. A barrier of several identical humps allows you to get how close the energy levels are, which leads to a transparency band, thereby increasing the integral current. Since the area of the usual barrier for metals is on the order of a few nanometers, the grid electrodes must have the same length, i.e. be transparent to electrons. The structures of carbon nanotube (CNT) and n-layer graphene sheets are very strong and meet all the requirements. It is convenient to use a grid of CNTs with a metallic type of conductivity, arranged collinearly in the plane, or to build grids of CNTs of the woodpile type. In the construction of grids, their fasteners are required fig. 1. In a triode structure with two grids, the first grid can be attached directly to the cathode, providing contact and the desired cathode potential on it. The second grid should be isolated and the specified voltage U_g applied to it. In this case, a three-humped potential barrier is formed. By placing several grids at the cathode potential, a quasi-periodic barrier can be formed. However, the "lowered" barrier is more promising, when several grids have the same pulling potential Fig. 2. Such a barrier can be transparent for some energies, Fig. 3, whereas for a two-hump barrier with a single grid, incomplete resonant tunneling usually occurs [8]. It is also convenient to consider the possibility of controlling the voltage of two grids at once, i.e., consider the tetrode and enter the potentials U_{1g} and U_{2g}.

2. Calculating the current density for an arbitrary barrier

Let the barrier be described by an arbitrary potential function $V(x)$. This function has a value $V(0)=-eU_0$ equal to the energy of the electrons at the bottom of the conduction band of the cathode. At the anode $V(d)=-e(U_0+U_a)$ is the energy of the electron at the bottom of the conduction band of the anode. The profile $V(x)$ has all negative values, while the free electron in a vacuum corresponds to zero kinetic energy. We also introduce the electron energy in the regions of two grids: $V_{1g}(x)=V(0)$ at $x_{1g}<x<x_{1g}+s_1$ and $V_{2g}(x)=-e(U_0+U_g)$ at $x_{2g}<x<x_{2g}+s_2$. In the intervals between the electrodes, the function changes continuously, but for the numerical solution of the SE, we divide these intervals by discrete points and use a stepwise representation of the potential function

$$V(x)=\sum_{j=1}^{N}V_j u_j(x). \qquad (1)$$

It is convenient to use unequal intervals to determine the unit step functions $u_j(x)=1$ at $x_{j-1}<x<x_j$, where V_j are the values of the potentials at the central points $\bar{x}_j=(x_{j-1}+x_j)/2$ of the steps defining the barrier. Namely, each grid electrode is described by a single step function. Each function corresponds to a transfer matrix

$$\hat{T}_j=\begin{bmatrix}\cos(k_j\Delta x_j) & -ik_j^{-1}\sin(k_j\Delta x_j)\\ -ik_j\sin(k_j\Delta x_j) & \cos(k_j\Delta x_j)\end{bmatrix}, \qquad (2)$$

in which $k_j=\sqrt{2m_e(E-V_j)}/\hbar$ for the above-barrier areas and $k_j=i\sqrt{2m_e(V_j-E)}/\hbar$ for the sub-barrier areas. Here m_e is the mass of the electron. Next, it is convenient to enter the designation $\mu=2m_e$. The program for solving SE consists in constructing a complete matrix $\hat{T}=\hat{T}_1\hat{T}_2...\hat{T}_N$ by multiplying the matrices of the regions and calculating the transmission coefficient from a system of equations $1+R=(T_{11}-iT_{12}/k)T$, $1-R=ik_0(T_{21}-iT_{22}/k)T$. Adding them together, we get the result $T=2/[T_{11}+T_{22}(k_0/k)+i(k_0T_{21}-T_{12}/k)]$, $R=1-k_0(T_{21}-iT_{22}/k)T$. Since we have $Z=(1+R)/(1-R)=(kT_{11}-iT_{12})/(ik_0kT_{21}+k_0T_{22})$, we can find the reflection coefficient from the barrier in another way: $R=(Z-1)/(Z+1)$. The calculated barrier transparency (tunneling) coefficient $D^+(E)=|T|^2$ depends on the kinetic energy E of the electron in the cathode region. The notations $k_0=\sqrt{\mu E}/\hbar$ and $k=\sqrt{\mu(E+eU_a)}/\hbar$ are used above, i.e. the values and are proportional to the electron pulses at the cathode and anode. The momentum of the electrons at the anode increases due to acceleration during the above-barrier movement. The incident flow of particles is determined by function $\exp(ik_0x)$, and the past flow is determined by function $\exp(ik_0x)$. Naturally, the hit of an electron on the anode leads to the relaxation of the additional pulse at about the free path length and to the heating of the anode. Usually, the electron energy is counted from the bottom of the conduction band, so the maximum kinetic energy (at zero temperature) is equal to the Fermi energy E_F. In this case, the depth of the cathode conduction band $V_c=eU_0=E_F+W_0$, and W_0 is the electron output work. Such barriers are constructed in Fig. 2. If the energy of the free electron is taken as the zero of the energy reference, then all the values of the energies and potentials will be negative. It is convenient to take the energy at the bottom of the conduction band of the anode as zero. Then the bottom of the conduction band of the cathode has a positive value eU_a, the maximum energy of the electron takes a

value $eU_a + E_F$, and all values V_j become positive and are counted from the "zero" potential of the anode. Such a potential profile is conveniently described by a sequence of rectangular steps. In all matrix elements there are differences that do not change due to a change in the reference frame. Either k_0 and k do not change. To calculate the current, we take into account study the electron energy distribution from the bottom of the conduction band to E_F, as well as the number of electrons incident with the corresponding normal component of the pulse on the barrier [2, 10]. Given this, the result for the current density at the cathode temperature T can be written as

$$J_e^+ = \frac{em_e^2 k_B T}{4\pi^2\hbar^3}\int_0^\infty D^+(E)\ln\left(1+\exp\left(\frac{m_e}{2k_B T}\left(v_F^2 - v^2\right)\right)\right)v\,dv,$$

and at zero temperature as

$$J_e^+ = \frac{em_e}{4\pi^2\hbar^3}\int_0^{E_F} D^+(E)(E_F - E)dE. \qquad (3)$$

At a low temperature, the expression (3) can be converted to the form

$$J_e^+ = \frac{em_e}{4\pi^2\hbar^3}\int_0^{E_F+k_B T} D^+(E)(E_F + k_B T - E)dE. \qquad (4)$$

3. Determining the barrier profile

The barrier profile is constructed by the method of multiple images [4–10], taking into account the fact that at a small distance δ from the conducting electrode and in the small region δ_g around the dielectric boundary, the image forces do not act. These dimensions of the order of Å can be associated with the work of the metal and dielectric exit [5–9]. The image method is suitable for barriers between two electrodes, taking into account the dielectric layers on their surfaces, i.e. images are used relative to several surfaces [4–9]. In the presence of a dielectric film on the cathode, there are three such surfaces, and, accordingly, the number of images is triple. For images relative to the surface of the dielectric, for the effective charge $q = -e/\varepsilon$ inside the dielectric, take the charge $q = e/\varepsilon$ of the image relative to the surface of the metal and $-e(\varepsilon-1)/(\varepsilon^2+\varepsilon)$ relative to the surface of the dielectric. For an electron $-e$ in a vacuum, the image relative to the surface of the dielectric is given by the charge $e(\varepsilon-1)/(\varepsilon+1)$. The image method immediately shows that the work on moving the charge in the film is about a factor ε less than the similar work without the

film (in a vacuum). The results of barrier modeling for structures with a film are given in [4–6]. The work on the transfer of a electron between the infinite plates of a flat capacitor with a size formed by the cathode and the first grid is determined by the potential function $W(x,\delta,\delta_g,g_1)$ [8-10]. It is

$$W=-\frac{e^2}{16\pi\varepsilon_0}\left\{\frac{1}{x+\delta}\left(1+\frac{2xg_1}{(g_1-x+\delta_g)(g_1+x)}\right)-\frac{2}{g_1}+\frac{2x^2}{g_1^3}\sum_{n=2}^{\infty}\frac{1}{\left(n^2-(x/g_1)^2\right)n}\right\}. \quad (5)$$

4. Emission control

Fig. 2 shows the profiles of a number of barriers, and Fig. 3 shows the calculations of the tunneling coefficient for the Fermi energy. For simple barriers, formula (9) and similar ones show that the maximum current is obtained for a cathode with a large concentration of electrons (Fermi energy) and a large transparency. Transparency can be adjusted by creating complex barriers. A large concentration of electrons is important for obtaining emission structures that can give off a large current density in extremely strong fields. All other things being equal, the emission current in the RTT depends on the grid potential. In fig. 3 shows the results of calculating the tunneling coefficient $D^+(E_F)$ from the grid voltage U_g. However, the maximum for resonance tunneling can be at lower energies, so it is important to calculate the total current density taking into account the energy distribution. This calculation is shown in Fig. 4 using formula (3). In this case, the integral was calculated numerically from 100 points of the quadrature formula of the averages, which required the calculation of 100 values $D^+(E_n)$.

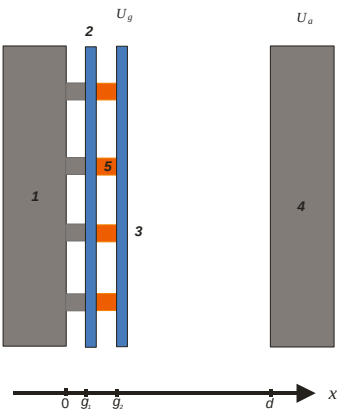

Fig. 1. Configuration in the form of a flat cathode 1, two grids 2, 3 of thickness s and a flat anode 4. The grid 2 contacts the cathode, 5 – dielectric fasteners of the insulated grid.

Рис. 1. Конфигурация в виде плоского катода 1, двух сеток 2, 3 толщиной s и плоского анода 4. Сетка 2 контактирует с катодом, 5 – диэлектрические крепления изолированной сетки

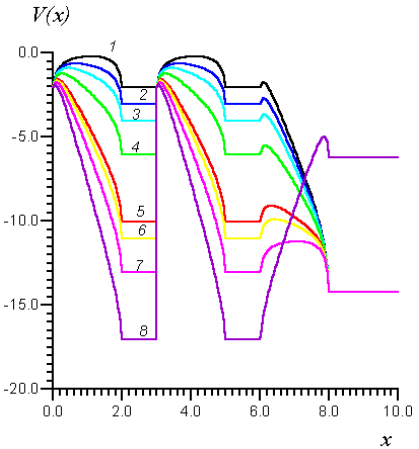

Fig. 2. Profiles of complex barriers in structures with two grids under the same potential (B): V_g = 0 (curve 1); 2 (2); 4 (3); 5 (4); 8 (5); 9 (6); 11 (7); 15 (8). V_a = 11 eV, d_1=d_2=d_3=2, s_1=s_2=1, δ = 0.1, δg = 0.15 (dimensions in nm). For curves 1–7 V_a = 11 eV, for curve 8 V_a = 5 eV.

Рис. 2. Профили сложных барьеров в структурах с двумя сетками при одном потенциале (В): Vg = 0 (кривая 1); 2 (2); 4 (3); 5 (4); 8 (5); 9 (6); 11 (7); 15 (8). Va = 11 эВ, d_1 = d_2 = d_3 = 2, s_1=s_2=1, δ= 0,1, δg = 0,15 (размеры в нм). Для кривых 1—7 Va = 11 эВ, для кривой 8 Va = 5 эВ

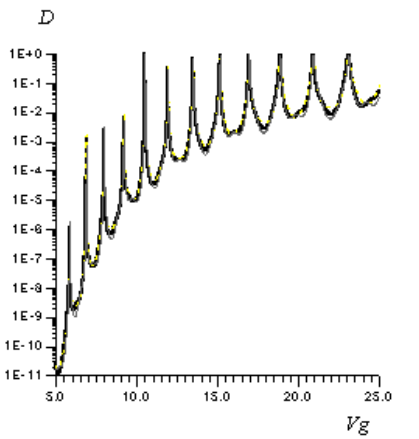

Fig. 3. The tunneling coefficient for the structure d_1 = d_2 = d_3 = 2, s_1 = s_2 = 1, δ = 0.1, δ_g=0.15 (nm) depending on the grid potential V_g (eV). V_a = 11 (eV).

Рис. 3. Коэффициент туннелирования для структуры d_1 = d_2 = d_3 = 2, s_1 = s_2 = 1, δ = 0.1, δ_g=0.15 (нм) в зависимости от потенциала сетки Vg (эВ). Va = 11 (эВ)

Although tunneling is usually described by a single-particle SE, in the sense there are particles falling on the barrier $N(E)=\psi^{+}(x,E)\psi^{+*}(x,E)$ with a density

in the flow at $x<0$, where the incident flow is described by a wave function $\psi^{+}(x,E)=a(E)\exp(ik_0x)$, and the reflected flow is described by a function $\psi^{-}(x,E)=Ra\exp(-ik_0x)$. Here also $k_0=\sqrt{\mu E}/\hbar$. The flow that passed into the anode is described by the function $Ta\exp(-ikx)$. The probability flows themselves have an expression $j(x,t)=\hbar(2m_ei)^{-1}\left(\psi^{*}(x,t)\partial_x\psi(x,t)-\psi(x,t)\partial_x\psi^{*}(x,t)\right)$. Due to the fact that the flow has an energy distribution, its wave function should be considered as a wave packet, represented as an energy integral. Formally, it is possible to construct static anode VAC and grid VAC and solve a non-stationary problem, considering the RTT in the circuit or as a concentrated element of a certain circuit. This problem for RTD is solved in [11]. The non-stationary dynamic problem is set as follows: until the moment $\underline{t}$ = 0 of tunneling, the tunneling is stationary, while the grid potential is constant (i.e., the barrier profile does not change), and the function $V(x)$ is determined as indicated above. If the flux density $jdE=m_e\left(2\pi^2\hbar^3\right)^{-1}(E_F-E)dE$ is high, the barrier profile may be affected by the electron density in the barrier region $\rho(x,E)=-e\psi(x,E)\psi^{*}(x,E)$, which should be determined from the solution of the one-dimensional Poisson equation (PE). If is the profile $V(x)$ obtained for a single electron, then the profile obtained taking into account the charge density will be denoted $\tilde{V}(x)$. The function can be determined based on the matrix approach given above, as well as by directly solving the SE $\partial_x^2\psi(x)=\mu\hbar^{-2}(V(x)-E)\psi(x)$. You can search for a similar solution in the barrier area in the form

$$\psi(x,E)=a(E)\left[(1+R(E))(1-x/d)+T(E)x/d\right]+\sum_{n=1}^{\infty}a_n\sin\left(\frac{n\pi x}{d}\right) \tag{8}$$

Substituting it in the SE, we get the equation for the coefficients

$$a_n(E)=\tilde{a}_n(E)+\left(E-\left(\frac{n\pi\hbar^2}{\mu d}\right)^2\right)^{-1}\sum_{m=1}^{\infty}V_{nm}a_m, \tag{9}$$

in which

$$\tilde{a}_n(E)=\frac{2a\int_0^d\left[(1+R)\left(1-\frac{x}{d}\right)+T\frac{x}{d}\right](V(x)-E)\sin\left(\frac{n\pi x}{d}\right)dx}{d\left(E-\left(n\pi\hbar^2\right)^2/(\mu d)^2\right)^{-1}},$$

$$V_{nm}=\frac{2}{d}\int_0^d V(x)\sin\left(\frac{n\pi x}{d}\right)\sin\left(\frac{m\pi x}{d}\right)dx.$$

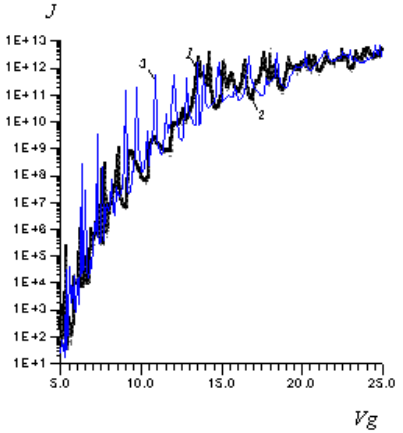

Fig. 4. Voltage-grid characteristics for the structure of Fig. 2 at different grid potential V_a: 11 eV (curve 1); 15 eV (2); 5 eV (3).

Рис. 4. Вольт-сеточные характеристики для структуры рис. 2 при различных потенциалах сетки *Va*: 11 эВ (кривая 1); 15 эВ (2); 5 эВ (3)

The wave function is continuous (”cross-linked") with the corresponding function outside the domain. However, you must also stitch the derivatives:

$$\left[1+ik_0(E)d\right]a(E)+a(E)R(E)\left[1-ik_0(E)d\right]=a(E)T(E)-\pi\sum_{n=1}^{\infty}na_n,$$

$$-a(E)\left(1+R(E)\right)+\pi\sum_{n=1}^{\infty}(-1)^n na_n=a(E)\left(1+ik_0(E)d\right)T(E).$$

These are additional conditions on the expansion coefficients. The given relations and the representation of the total wave function in the form of a spectral integral allow us to define the total fluxes of the probability density $j(x,t)=\hbar(\mu i)^{-1}\left(\psi^*(x,t)\partial_x\psi(x,t)-\psi(x,t)\partial_x\psi^*(x,t)\right)$. The input stream $j(0,t)$ is stationary.

Let the grid voltage $U_g(t)$ begin to change at the moment t=0. Generally speaking, this leads to a change in the entire profile $V(x,t)$, and the wave function must satisfy the non-stationary SE. The nonstationary SE solution should be consistent with the boundary conditions at the cathode. Inside the cathode, the electrons are free, and the wave function is a wave packet

$$\psi(x,t)=\int_0^{E_F}a(E)\left[\exp(ik_0x)+R(E)\exp(-ik_0x)\right]\exp(-iEt/\hbar)dE.$$

Calculating the probability flow, we have

$$j(x,t)=\frac{\hbar}{m_e}\int_0^{E_F}k_0(E)a^2(E)\left(1-\left|R(E)\right|^2\right)dE.$$

For incoming electrons $a^2(E)=m_e^2(E_F-E)/(2\pi^2\hbar^4k_0)$. The input current is stationary and is equal to $J=-ej(0,t)=-ej(0,0)$. We define a function $\tilde{V}(x)=V(x)-e\tilde{U}(x)$ where the potential $\tilde{U}(x)$ satisfies the PE $\partial_x^2\tilde{U}(x)=-\rho(x)/\varepsilon_0$ with zero boundary conditions at the cathode and anode. We are looking for the specified solution in the form

$$\tilde{U}(x)=\sum_{n=1}^{\infty}u_n\sin(n\pi x/d),$$

where do we get the expansion coefficients from

$$u_n=\frac{-2ed}{\varepsilon_0 n^2\pi^2}\int_0^d|\psi(x)|^2\sin\left(\frac{n\pi x}{d}\right)dx.$$

In the non-stationary case time-dependent wave function $\psi(x,t)$ and potentials $V(x,t)$, $\tilde{V}(x,t)$ and $\tilde{U}(x,t)$ should be used. We assume that at the moment t = 0 the initial conditions of the type $\psi(x,0)=\psi(x)$, $V(x,0)=V(x)$, etc. are satisfied. For each moment of time, it is necessary to jointly solve the SE with the function $\tilde{V}(x,t)$ and the PE with the charge density $-e|\psi(x,t)|^2$. It is convenient to assume that $U_g(t)=U_{g0}+\Delta U_g(t)$ at $t>0$ and $V(x,t)=V(x)$ off the grid, for example, $U_g(t)=U_{g0}(1+k\sin(\omega_0 t))$. Then $V(x,t)=V(x)-e\Delta U_g(t)$. A change in the potential function in a small region leads to a change in the wave function in the entire region: $\psi(x,t)=\psi(x)+\delta\psi(x,t)$. Substituting this function in the SE with replacement $V(x)$ by $\tilde{V}(x)$ and taking into account the stationary SE, which satisfies $\psi(x)$, we obtain

$$i\hbar\partial_t\delta\psi(x,t)=\left(-\frac{\hbar^2\partial_x^2}{\mu}+\tilde{V}(x)\right)\delta\psi(x,t)-e\Delta U_g(t)\psi(x,t), \tag{10}$$

As a result of solving SE in the first approximation, we have (see [11])

$$J(d,t)=J(d,0)+2e\hbar\left(d-g_2-\frac{s}{2}\right)\alpha\int_0^t\frac{\cos\left(\frac{\mu(x-g_2-s/2)^2}{2|t-t'|}+\varphi_0-\varphi_d-\frac{3\pi}{4}\right)}{(t-t')^{3/2}}\Delta U_g(t')dt', \tag{11}$$

Here $\varphi_0=\varphi(g_2+s/2)$, $\varphi_d=\varphi(d)$ are the phases of wave function.

5. Conclusions

Stationary and non-stationary RTT models are proposed in this paper. To create a potential barrier profile with several maxima, including quasi-periodic profiles, it is proposed to use additional grid electrodes. Part of the grid elec-

trodes can be located at the cathode potential. Then the introduction of the control electrode implements RTT. The complex profile of the barrier in the work is determined by the method of multiple images. The matrix method is used to solve the SE, and the series method is proposed, which allows us to solve both the SE and the PE together. It is shown that there is a grid potential at which the barrier is transparent, and that there is a falling section of the grid characteristic. A non-stationary RTT model is proposed, which allows calculating the dynamic current-voltage characteristics. In this case, a linear approximation and a nonlinear equation of the current-voltage dependence on the label are obtained.

Fig. 3 and 4 show that the grid current-voltage characteristics when performing resonant tunneling (at a high voltage on the grid) are weakly dependent on the anode voltage. Performing the anode in the form of a grid in this mode and using an accelerating electrode behind it, it is possible to obtain a high-current electron beam of high density, which is orders of magnitude higher than the usually achievable densities for planar cathodes with coatings of diamond-graphite clusters.

Acknowledgment

This work was supported by grant from the Ministry of Education and Science of the Russian Federation within the framework of the State task (project No. FSRR-2020-0004).

References

1. Fursey G. N. Field emission in vacuum micro-electronics. NY : Kluwer Academic Plenum Publishers ; Springer, 2005. 205 p.
2. Проскуровский Д. И. Эмиссионная электроника. Томск : ТГУ, 2010. С. 154–233.
3. Forbes R. G., Xanthakis J. P., Low-macroscopic-field electron emission from carbon films and other electrically nanostructured heterogeneous materials : hypotheses about emission mechanism // Solid-State Electronics. 2001. Vol. 45, No. 6. P. 779–808.
4. Davidovich M. V., Yafarov R. K., Doronin D. M. Electron tunneling in the presence of dielectric film on the cathode. In : 2011 21st International Crimean Conference “Microwave & Telecommunication Technology” (CriMiCo’2010). Sevastopol, 2010. P. 733–734.
5. Davidovich M. V., Bushuev N. A. Field Emission in Diode and Triode Vacuum Nanostructures. In : 2014 Tenth International Vacuum electron Sources Conference and Second International Conference on Emission Electronics. Saint-Petersburg, Saint-Petersburg State University, 2014. P. 58–59.
6. Davidovich M. V., Bushuev N. A., Yafarov R. K. Tunnel Current in the Presence of Nanosized Film at the Cathode. In : 2014 Tenth International Vacuum electron Sources Conference and Second International Conference on Emission Electronics, Saint-Petersburg, Saint-Petersburg State University, 2014. P. 67–68.
7. Davidovich M. V., Bushuev N. A. The field emission electron gun with wide and thin ribbon bean. In : 25th Int. Crimean Conf. “Microwave and Telecommunication Technology” (CriMiCo’2015). Sevastopol, 2015. P. 145–146.
8. Davidovich M. V., Yafarov R. K. Pulse and static field emission VAC of carbon nanoclaster structures: experiment and its interpretation // Technical Physics. 2019. Vol. 64, No. 8. P. 1210–1220.

9. Davidovich M. V., Yafarov R. K. Field-emission staggered structure based on diamond-graphite clusters // Technical Physics. 2018. Vol. 63, No. 2. P. 274–284.
10. Simmons J. G. Generalized formula for the electric tunnel effect between similar electrodes separated by a thin insulating film // J. Appl. Phys. 1963. Vol. 34, No. 6. P. 1793–1803.
11. Davidovich M. V. Time-dependent resonant tunneling in a double-barrier diode structure // Jetp Lett. 2019. Vol. 110. P. 472–480.

Information about the authors

Michael V. Davidovich, Dr. Sci., Professor, Professor of the Department of Radio Engineering and Electrodynamics of the Institute of Physics, Saratov National Research State University named after N. G. Chernyshevsky, Russian Federation. ORCHID 0000-0001-8706-8523.

German N. Kolesov, engineer, postgraduate student, RFNC-VNIIEF, Sarov, Russian Federation.

Kirill A. Sayapin, Engineer, Institute of Physics, Saratov National Research State University n. a. N. G. Chernyshevsky.

Информация об авторах

Давидович Михаил Владимирович, доктор физико-математических наук, профессор, профессор кафедры радиотехники и электродинамики Института физики Саратовского национального исследовательского государственного университета им. Н. Г. Чернышевского. ORCID 0000-0001-8706-8523.

Колесов Герман Николаевич, инженер, аспирант, РФЯЦ-ВНИИЭФ, г. Саров Нижегородской области.

Саяпин Кирилл Александрович, инженер Института физики Саратовского национального исследовательского государственного университета им. Н. Г. Чернышевского.